Modulation of Metarhodopsin Formation by Cholesterol-Induced Ordering of Bilayer Lipids†

Drake C. Mitchell, Martin Straume,‡ James L. Miller,§ and Burton J. Litman*
Department of Biochemistry, University of Virginia Health Sciences Center, Charlottesville, Virginia 22908
Received March 15, 1990; Revised Manuscript Received July 9, 1990

ABSTRACT: The effect of lipid ordering on the kinetics and extent of metarhodopsin II (meta II) formation was evaluated in bovine rhodopsin which had been reconstituted into phosphatidylcholine vesicles containing 0, 15, and 30 mol % cholesterol. The rate of establishment of the dynamic equilibrium between metarhodopsin I (meta I) and the two kinetically distinguished forms of meta II in the branched meta II model [meta II_{fast} and meta II_{slow}; Straume, M., Mitchell, D. C., Miller, J. L., & Litman, B. J. (1990) *Biochemistry* (preceding paper in this issue)] is derived from kinetic measurements of rhodopsin photolysis in these vesicle systems at several temperatures. Values of the meta I ↔ meta II_{total} equilibrium constant, K_{eq}, are calculated from the derived model-dependent rate constants, and are shown to be equivalent to those derived from rapidly acquired absorbance spectra. The presence of 30 mol % cholesterol reduces K_{eq} by approximately 50% between 10 and 37 °C. Analysis of the model-dependent parameters in terms of ΔH and ΔS reveals that cholesterol raises the free energy of meta II_{slow}, relative to meta I, by increasing ΔH whereas it raises the relative free energy of meta II_{fast} by making ΔS of meta II_{fast} relative to meta I less positive. The reduction in K_{eq} by both temperature and cholesterol is found to be directly correlated with a parameter that reflects the free volume available for molecular motion in the hydrophobic core of the bilayer [Straume, M., & Litman, B. J. (1988) *Biochemistry 27*, 7723–7733]. This correlation is interpreted as evidence that meta II formation is modulated by the packing properties of the surrounding lipid bilayer rather than by any specific rhodopsin–lipid interactions. Such modification of the functional competence of an integral membrane protein by variation of the lipid bilayer composition provides a potential control mechanism in the essentially isothermal environment of living cells. The implications of the results for the nature of the meta I to meta II transition and for the role of the lipid bilayer in visual signal transduction are discussed.

The visual pigment rhodopsin is representative of a class of integral membrane protein receptors that utilize guanine nucleotide binding proteins (G-proteins) to couple extracellular stimuli to the regulation of intracellular effector enzymes. Unlike other receptors in this group, the protein portion of rhodopsin has covalently bound to it a retinal moiety. Conformation changes in the vicinity of this retinal chromophore following photoexcitation may be kinetically monitored with nonperturbative optical techniques. Such studies show that within a few milliseconds of photon absorption, bleached rhodopsin exists in an equilibrium between two spectrally defined intermediates: metarhodopsin I (meta I)[1] (λ_{max} = 478 nm) and meta II (λ_{max} = 380 nm) (Mathews et al., 1963). Meta II formation is of particular interest because this species is spectrally identical with the agonist-bound form of rhodopsin (rho*) which catalyzes activation of G_t, the G-protein in the rod outer segment (Emeis et al., 1982). In visual signal transduction, the first step in the transfer of stimulus from the receptor, rhodopsin, to the rod cell plasma membrane sodium channels is the binding and subsequent activation of G_t by rho*. The ability to kinetically resolve the formation of agonist-bound receptor by monitoring changes in the retinal absorption spectrum makes rhodopsin ideal for studying the relationship between lipid bilayer properties and integral membrane protein receptor activation and function.

Interactions between the transmembrane domain of rhodopsin and its hydrophobic environment play a major role in determining the stability of rhodopsin and several of its photochemical intermediates. The disk membrane phospholipid bilayer has been shown to play a major role in stabilizing the native conformation of opsin (Stubbs & Litman, 1978a,b), and the effect of the lipid bilayer on the formation of meta II has been examined under a variety of conditions. The rate of meta II formation is greatly increased following solubilization of rhodopsin in detergent micelles (Applebury et al., 1974; Litman et al., 1981). Meta II formation is also enhanced when rhodopsin is incorporated into phospholipid bilayers containing increasing levels of fatty acid unsaturation (O'Brien et al., 1977). In contrast, rhodopsin incorporated into saturated dimyristoylphosphatidylcholine vesicles shows a reduced ability to form meta II, particularly when the bilayer is in the gel state (Mitchell et al., 1990).

The present work extends the previous investigations in two important ways. First, application of the photoreaction model shown in Figure 1 and the analytical approach described by Straume et al. (1990, preceding paper in this issue) makes it possible to completely characterize all photochemical activity on the meta I–meta II time scale. This level of analytical treatment facilitates interpretation of the kinetics of establishment of the meta I ↔ meta II equilibrium in a physically meaningful manner. Second, the effect of isothermal per-

†Supported by NIH Grant EY00548 and NSF Grant PCM-8316858. A preliminary report of this work appeared in Mitchell et al. (1989).
*Address correspondence to this author.
‡Present address: Biocalorimetry Center, Department of Biology, The Johns Hopkins University, Baltimore, MD 21218.
§Present address: Department of Physiology, University of California, San Francisco, San Francisco, CA 94143.

[1] Abbreviations: meta I, metarhodopsin I; meta II, metarhodopsin II; DPH, diphenylhexatriene; DTPA, diethylenetriaminepentaacetic acid; DTT, dithiothreitol; G_t, visual G-protein, GTPase of the rod outer segment, transducin; PC, phosphatidylcholine; PIPES, piperazine-*N*,*N*′-bis(ethanesulfonic acid); ROS, rod outer segment.

0006-2960/90/0429-9143$02.50/0

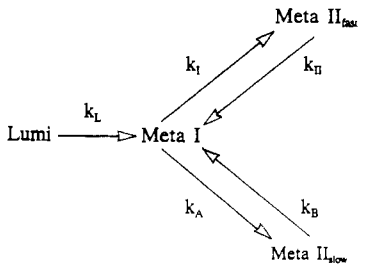

FIGURE 1: Branched meta II model of the lumi–meta I–meta II portion of the rhodopsin photoreaction cascade. For a detailed discussion, see Straume et al. (1990).

turbation of the physical properties of a phospholipid bilayer on meta II formation can be determined by incorporating rhodopsin into phospholipid bilayer vesicles of varying cholesterol content. Altering bilayer acyl chain order by varying the composition of the bilayer mimics the conditions in the near-isothermal environment of the cell, where the properties of integral membrane proteins (e.g., receptors and channels) may be modulated by adjusting the membrane composition, but not via large changes in temperature. Examination of these reconstituted systems as a function of temperature has made it possible to uncouple the distinct effects of temperature and variation in bilayer composition on the ordering of bilayer phospholipids (Straume & Litman, 1988). The use of such systems in these studies has facilitated the independent assessment of the effect of both temperature and compositionally induced ordering on the two meta I ↔ meta II equilibria. These results are correlated with a parameter related to the volume available for molecular motion in the hydrophobic portion of the bilayer, derived from fluorescence depolarization studies (Straume & Litman, 1988).

Experimental Procedures

Large, unilamellar egg PC vesicles containing 0, 15, or 30 mol % cholesterol and purified rhodopsin were prepared by an octyl glucoside dilution method as described by Jackson and Litman (1985) with the modifications of Straume and Litman (1988) regarding the inclusion of cholesterol. Egg PC was purchased from Avanti Polar Lipids Inc. (Birmingham, AL), and cholesterol was purchased from Calbiochem (La Jolla, CA). All buffers and solutions were saturated with argon and contained 50 μM DTPA and 62.5 μM $MgCl_2$ to minimize lipid peroxidation catalyzed by trace amounts of iron.

Total cholesterol content was determined by a cholesterol oxidase assay (Moore et al., 1977) and was always within 1 mol % of the desired 15 and 30 mol % levels. Total protein, phospholipid, and unbleached rhodopsin concentrations were determined as previously described [see Straume et al. (1990) and references cited therein].

Samples were prepared from a concentrated vesicle stock suspension by dilution with concentrated, temperature-compensated buffer. Final rhodopsin suspensions were 0.2–0.4 mg/mL rhodopsin in pH 7.0 PIPES buffer which consisted of 10 mM PIPES, 60 mM KCl, 30 mM NaCl, 2 mM $MgCl_2$, 2 mM DTT, and 50 μM DTPA. Samples for equilibrium spectral measurements consisted of aliquots of the samples used for kinetic measurements.

The kinetics of meta I, meta II_{fast}, and meta II_{slow} formation were derived by analyzing kinetic absorbance data acquired at 380 nm in terms of a branched meta II model (Figure 1). A nonlinear least-squares parameter estimation procedure was used to derive explicit values of all five rate constants (k_L, k_I, k_{II}, k_A, and k_B) and the contribution of each species to the absorbance increase at 380 nm, and to determine the uncertainty in each of these quantities corresponding to one standard deviation. $K_{eq,total}$, $K_{eq,fast}$, and $K_{eq,slow}$ were calculated from the resulting forward and reverse rate constants, and uncertainties corresponding to one standard deviation were linearly propagated from those of the rate constants. Details of the analytical methods used to obtain the individual rate constants and amplitudes of lumirhodopsin, meta I, meta II_{fast}, and meta II_{slow}, and the methods used to derive equilibrium meta I–meta II spectra are given in Straume et al. (1990).

Absorbance spectra of the meta I ↔ meta II equilibrium mixture were derived from a series of four spectrophotometer scans obtained from the same sample. These scans were of (1) the starting material, (2) 2–5 s after a brief green flash delivered to the previously unbleached material, (3) following addition of hydroxylamine to (2), and (4) after complete bleaching of (3). Distinct, individual absorbance spectra of meta I and meta II were derived from the spectrum of their equilibrium mixture using nonlinear least-squares parameter estimation. K_{eq} was calculated from the individual spectra by using extinction coefficients of 44 000 M^{-1} cm^{-1} for meta I at 478 nm and 38 000 M^{-1} cm^{-1} for meta II at 380 nm (Applebury, 1984).

The activation enthalpy and entropy for each rate process were obtained by using nonlinear least squares to analyze the temperature dependence of each rate constant in terms of the equation:

$$k = k_B T/h \exp(\Delta S^{\ddagger}/R) \exp(-\Delta H^{\ddagger}/RT) \quad (1)$$

where k_B is Boltzmann's constant, T is the absolute temperature, h is Planck's constant, R is the universal gas constant, $\Delta S^{\ddagger}$ is the molar activation entropy, and $\Delta H^{\ddagger}$ is the molar activation enthalpy.

Changes in enthalpy and entropy associated with the meta I ↔ meta II_{total} equilibrium and the separate meta I ↔ meta II_{fast} and meta I ↔ meta II_{slow} equilibria were determined by using nonlinear least-squares parameter estimation to analyze the temperature dependence of each equilibrium in terms of the equation:

$$K_{eq,species} = \exp(\Delta S_{species}/R) \exp(-\Delta H_{species}/RT) \quad (2)$$

where "species" refers to meta II_{fast}, meta II_{slow}, or meta II_{total} and ΔH and ΔS are the changes in enthalpy and entropy, respectively, relative to meta I. Changes in free energy at 25 °C, ΔG_{25}, were determined by using an equation similar to eq 2, except ΔS was exchanged for the quantity $(\Delta H - \Delta G_{25})/298.15$. This permitted direct estimation of the uncertainty associated with each parameter of interest.

Results

An example of cholesterol-induced changes in the meta I ↔ meta II equilibrium, under isothermal conditions, is presented in Figure 2. The time course of the absorbance increase at 380 nm for 0, 15, and 30 mol % cholesterol at 30 °C is represented by the data sets labeled a, b, and c, respectively. Each of the solid curves in Figure 2 represents the best fit of the branched meta II model (see Figure 1) to the corresponding data set. The residuals for each data set are shown in the inset panels and demonstrate that the kinetics of the formation of the meta I ↔ meta II equilibrium in these reconstituted bilayers are well described by the model. The three data sets in Figure 2 were normalized with respect to the concentration of photolyzed rhodopsin, so that the amplitudes of the transients can be directly compared. These data demonstrate that increasing bilayer cholesterol slows the growth and reduces the magnitude of the absorbance transient at 380 nm. However, evaluation of the derived parameters is necessary for an understanding of how a reduction of 380-nm

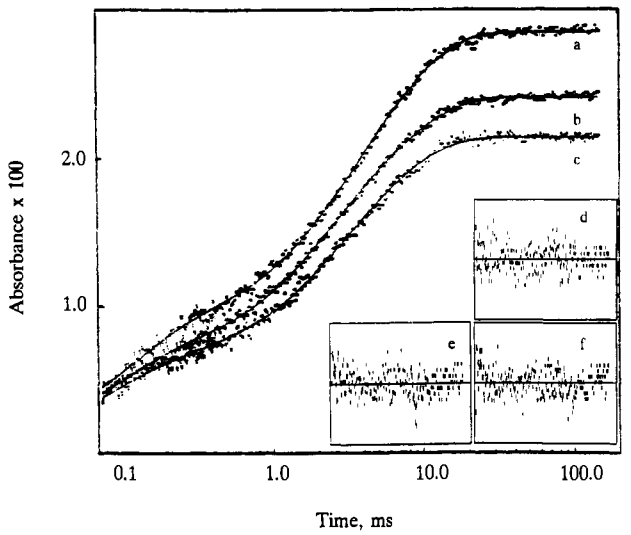

FIGURE 2: Observed increase in absorbance at 380 nm for photolyzed rhodopsin in egg PC vesicles containing 0 (a), 15 (b), and 30 mol % (c) cholesterol. Vesicles suspended in pH 7.0 PIPES buffer at 30 °C. Observed data are shown as points; solid curves are best fit of branched meta II model to the data. Inset panels are residuals for 0 (d), 15 (e), and 30 mol % (f) cholesterol.

Table I: Dependence of the Rate Constants Derived from the Branched Meta II Model on Bilayer Cholesterol Content at 37 °C[a]

rate constant	0 mol % cholesterol	15 mol % cholesterol	30 mol % cholesterol
k_L	13.7 ± 0.7	15.61 ± 0.42	17.92 ± 0.16
k_I	0.140 ± 0.003	0.145 ± 0.02	0.093 ± 0.013
k_{II}	0.739 ± 0.029	0.92 ± 0.07	1.01 ± 0.02
k_A	0.129 ± 0.015	0.122 ± 0.009	0.113 ± 0.004
k_B	0.157 ± 0.007	0.211 ± 0.014	0.247 ± 0.009

[a] Values of the rate constants and uncertainties corresponding to one standard deviation derived as described under Experimental Procedures. All rate constants are ms^{-1}.

absorbance relates to a shift in the meta I ↔ meta II equilibrium.

The effect of cholesterol on the derived rate constants of the branched meta II model at 37 °C is summarized in Table I. At this temperature, the rate of formation of meta II_{fast}, k_I, was essentially unchanged in the 15 mol % cholesterol bilayer, but significantly decreased in the 30 mol % bilayer, and the rate of meta II_{slow} formation, k_A, was only slightly reduced with increasing bilayer mole percent cholesterol. The rate constants most affected by the presence of cholesterol were k_{II} and k_B, the reverse rates for meta II_{fast} and meta II_{slow}, respectively, which were progressively larger with increasing bilayer mole percent cholesterol. Thus, at 37 °C, the equilibrium concentration of meta II declines with increasing bilayer mole percent cholesterol due largely to augmented reverse rates for both forms of meta II.

The effect of temperature on the model-dependent rate constants in the 0, 15, and 30 mol % cholesterol bilayers is illustrated in Figure 3A–C. The quantity log (k_i/T) is plotted against $1000/T$, the linearized form of eq 1, producing slopes proportional to $\Delta H^{\ddagger}$ and intercepts proportional to $\Delta S^{\ddagger}$. The straight lines in all three panels demonstrate that all of the model-dependent rate constants are well characterized by eq 1 over the range of temperature and bilayer compositions studied. The figures for 0 and 30 mol % cholesterol (panels A and C, respectively) are significantly different: in Figure 3C, the plots for k_I and k_B are nearly parallel, and the slope of k_A is much greater than the slope for any other rate constant. The figures for 0 and 15 mol % cholesterol (panels A and B, respectively) are quite similar, indicating that 15 mol % cholesterol has less of an effect than 30 mol % cholesterol on $\Delta S^{\ddagger}$ and $\Delta H^{\ddagger}$ of the model-dependent rate constants.

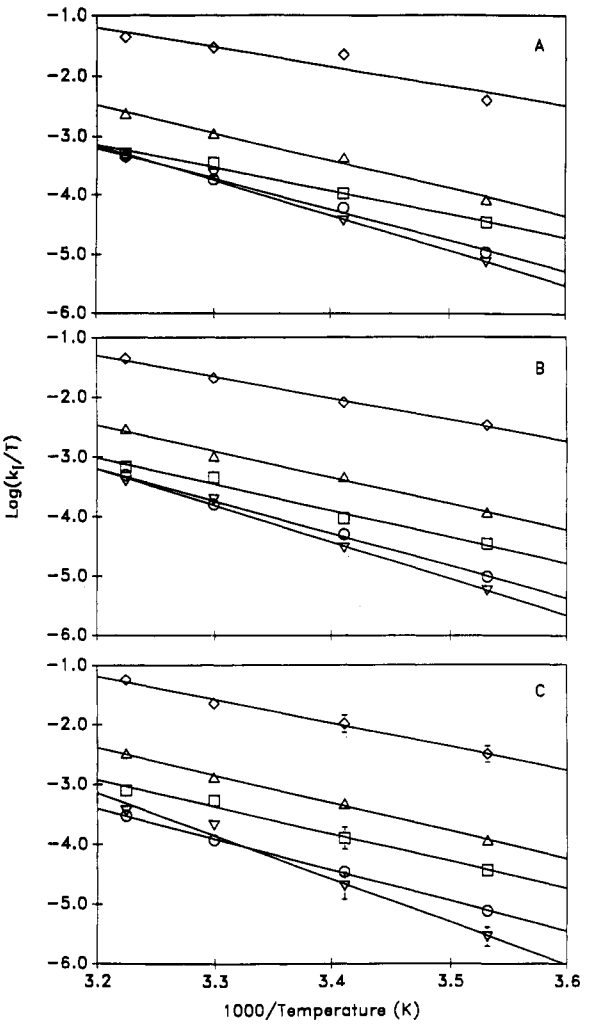

FIGURE 3: Temperature dependence of model rate constants in 0 (A), 15 (B), and 30 mol % (C) cholesterol, plotted according to linearized form of eq 1. Rate constants: k_L (◇), k_I (○), k_{II} (△), k_A (▽), k_B (□).

Table II: Dependence of $\Delta H^{\ddagger}$ and $\Delta S^{\ddagger}$ on Bilayer Cholesterol Content[a]

rate constant	mol % cholesterol	$\Delta H^{\ddagger}$ (kcal/mol)	$\Delta S^{\ddagger}$ [cal/(mol·K)]
k_L	0	15.6 ± 0.9	10.9 ± 2.5
	15	16.8 ± 2.0	14.4 ± 6.2
	30	18.3 ± 2.7	19.5 ± 6.8
k_I	0	24.0 ± 0.4	28.7 ± 1.5
	15	24.1 ± 1.6	29.0 ± 4.5
	30	24.7 ± 0.5	30.7 ± 1.8
k_{II}	0	18.5 ± 1.2	13.1 ± 3.9
	15	20.9 ± 0.5	22.1 ± 2.1
	30	22.6 ± 0.4	27.9 ± 1.8
k_A	0	27.2 ± 1.4	39.1 ± 4.8
	15	28.6 ± 1.6	43.2 ± 6.3
	30	32.9 ± 3.9	57.7 ± 12.9
k_B	0	18.0 ± 1.1	9.8 ± 4.0
	15	19.9 ± 1.2	16.3 ± 5.6
	30	20.8 ± 1.7	19.8 ± 9.1

[a] Values of $\Delta H^{\ddagger}$ and $\Delta S^{\ddagger}$ and uncertainties derived as described under Experimental Procedures.

The changes in $\Delta S^{\ddagger}$ and $\Delta H^{\ddagger}$ associated with each rate constant in 0, 15, and 30 mol % cholesterol are presented in Table II. Both $\Delta S^{\ddagger}$ and $\Delta H^{\ddagger}$ for k_{II}, k_A, and k_B were significantly altered by the presence of cholesterol, while for k_I these parameters were only somewhat affected. In all cases,

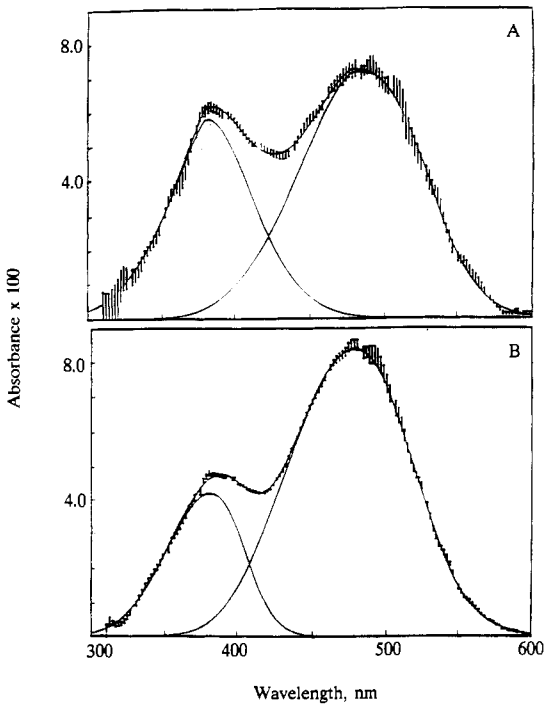

FIGURE 4: Equilibrium meta I–meta II spectra for photolyzed rhodopsin in egg PC vesicles containing 0 (A) and 30 mol % (B) cholesterol. Vesicles suspended in pH 7.0 PIPES buffer at 30 °C. Derived difference spectra shown as points with associated uncertainty; solid curve through points is best fit of the sum of two asymmetric, quasi-Gaussian functions to the difference spectra [for details, see Straume et al. (1990)]. Deconvoluted individual spectra of meta I and meta II shown as solid curves.

30 mol % cholesterol caused greater changes than 15 mol % cholesterol. Cholesterol raised $\Delta S^{\ddagger}$ for all four of these rate constants, indicating that bilayer cholesterol decreased the stearic or orientational requirements for formation of the respective transition states. In contrast, increased bilayer mole percent cholesterol increased $\Delta H^{\ddagger}$ for all four rate constants. The resulting balance between competing changes in $\Delta H^{\ddagger}$ and $T\Delta S^{\ddagger}$ was such that increased bilayer mole percent cholesterol generally raised $\Delta G^{\ddagger}$ for the two forward rates, k_{I} and k_{A}, and decreased $\Delta G^{\ddagger}$ for the reverse rates, k_{II} and k_{B}, at all temperatures.

The equilibrium mole fractions of meta I, meta $\mathrm{II}_{\mathrm{fast}}$, and meta $\mathrm{II}_{\mathrm{slow}}$ and K_{eq} were calculated from the derived forward and reverse rate constants. All values of K_{eq} calculated in this manner were compared with those derived from analysis of equilibrium spectral data. Typical equilibrium spectral data for the 0 and 30 mol % cholesterol bilayers are presented in panels A and B, respectively, of Figure 4. The curve through the data represents the best nonlinear least-squares fit to the spectral data of the sum of two asymmetric quasi-Gaussian functions, one corresponding to meta I and the other to meta II. These individual meta I and meta II spectra are also shown. The data are normalized in terms of the amount of photolyzed rhodopsin to clearly illustrate the degree to which 30 mol % cholesterol inhibits the formation of meta II. All values of K_{eq} derived from both the equilibrium spectral data and the kinetic data agree within their associated errors, as shown in Table III. Values of K_{eq} derived from the kinetic data will be used in all subsequent calculations and discussion.

The branched meta II model divides meta II into meta $\mathrm{II}_{\mathrm{fast}}$ and meta $\mathrm{II}_{\mathrm{slow}}$, and each of these species is postulated to exist in equilibrium with meta I (Straume et al., 1990). The changes in ΔH, ΔS, and ΔG_{25} for meta $\mathrm{II}_{\mathrm{fast}}$, meta $\mathrm{II}_{\mathrm{slow}}$, and meta $\mathrm{II}_{\mathrm{total}}$ in the three bilayers are given in Table IV. This

Table III: Values of K_{eq} from Kinetic and Equilibrium Spectral Measurements[a]

temp (°C)	mol % cholesterol	K_{eq}(kinetic)	K_{eq}(equilibrium)
10	0	0.35 ± 0.06	0.31 ± 0.04
	15	0.25 ± 0.03	0.26 ± 0.05
	30	0.15 ± 0.03	0.15 ± 0.04
20	0	0.49 ± 0.06	0.54 ± 0.05
	15	0.43 ± 0.05	0.45 ± 0.05
	30	0.25 ± 0.03	0.23 ± 0.04
30	0	0.78 ± 0.03	0.81 ± 0.06
	15	0.59 ± 0.06	*b*
	30	0.48 ± 0.03	0.51 ± 0.05
37	0	1.01 ± 0.1	1.21 ± 0.08
	15	0.75 ± 0.06	*b*
	30	0.55 ± 0.03	0.60 ± 0.06

[a] Values of K_{eq} and uncertainties derived as described under Experimental Procedures. [b] Not measured.

Table IV: Dependence of ΔH, ΔS, and ΔG_{25} for Meta $\mathrm{II}_{\mathrm{fast}}$ and Meta $\mathrm{II}_{\mathrm{slow}}$ on Bilayer Cholesterol Content[a]

	mol % cholesterol	ΔH (kcal/mol)	ΔS [cal/(mol·K)]	ΔG_{25} (kcal/mol)
meta $\mathrm{II}_{\mathrm{fast}}$	0	3.8 ± 0.8	8.8 ± 1.7	1.18 ± 0.05
	15	3.0 ± 0.7	5.9 ± 0.9	1.22 ± 0.03
	30	2.3 ± 1.0	2.6 ± 1.0	1.53 ± 0.05
meta $\mathrm{II}_{\mathrm{slow}}$	0	9.8 ± 0.7	31.5 ± 1.1	0.45 ± 0.03
	15	10.1 ± 0.8	32.0 ± 1.5	0.57 ± 0.03
	30	11.9 ± 1.0	37.0 ± 3.3	0.86 ± 0.05
meta $\mathrm{II}_{\mathrm{total}}$	0	8.2 ± 0.5	26.6 ± 0.8	0.29 ± 0.02
	15	8.5 ± 0.8	27.2 ± 1.0	0.39 ± 0.02
	30	9.4 ± 0.9	29.3 ± 1.5	0.68 ± 0.04

[a] Values of ΔH, ΔS, and ΔG_{25} and uncertainties derived as described under Experimental Procedures.

table shows that cholesterol progressively raises the total free energy of both meta II species relative to meta I. However, the changes in ΔH and ΔS which cause these increases in ΔG_{25} are very different for the two species. In the case of meta $\mathrm{II}_{\mathrm{fast}}$, in the presence of 30 mol % cholesterol, ΔH is reduced by ca. 40% while ΔS is reduced by ca. 70%. In contrast, 30 mol % cholesterol produces the opposite changes for meta $\mathrm{II}_{\mathrm{slow}}$; both ΔH and ΔS are increased by ca. 20%. As a result of these changes, cholesterol alters the division of meta II between meta $\mathrm{II}_{\mathrm{fast}}$ and meta $\mathrm{II}_{\mathrm{slow}}$. In the 0 mol % cholesterol bilayer, the equilibrium ratio [meta $\mathrm{II}_{\mathrm{slow}}$]/[meta $\mathrm{II}_{\mathrm{fast}}$] varies from 1.5 at 10 °C to ca. 30 at 37 °C. However, in the 30 mol % cholesterol bilayer, this ratio varies from 1.1 at 10 °C to only 3.5 at 37 °C. The underlying thermodynamic basis for the reduction in $K_{\mathrm{eq,total}}$ with increasing bilayer cholesterol is demonstrated by the values of ΔH and ΔS for meta $\mathrm{II}_{\mathrm{total}}$, shown in Table IV. Increasing the mole percent cholesterol in the bilayer increases ΔS, which would augment the equilibrium concentration of meta $\mathrm{II}_{\mathrm{total}}$, but the relatively larger increase in ΔH results in suppression of meta $\mathrm{II}_{\mathrm{total}}$. Thus, cholesterol reduces the equilibrium concentration of meta $\mathrm{II}_{\mathrm{total}}$ by increasing the enthalpy of this state relative to meta I.

Discussion

Results of both the kinetic and equilibrium spectral experiments clearly establish that the equilibrium concentration of meta II is reduced as bilayer mole percent cholesterol is increased. Analysis of the kinetic observations in terms of the branched meta II model (Figure 1) produced values of K_{eq} which agree with those derived from the equilibrium spectral data (Table III), demonstrating that this model constitutes an accurate, quantitative description of the meta I ↔ meta II equilibrium in these reconstituted systems. Cholesterol altered all of the model-dependent rate constants, generally

decreasing the rates of meta I decay (k_I and k_A) and increasing the rates of back-reaction to meta I (k_{II} and k_B). As a result, the principle consequence of increased bilayer cholesterol was a reduction in the equilibrium concentration of both meta II_{fast} and meta II_{slow}. Cholesterol had a more pronounced effect on meta II_{slow} than on meta II_{fast}. In the bilayers containing 30 mol % cholesterol, the percentage of equilibrium meta II present as meta II_{slow} was significantly reduced, and the effect was more pronounced at higher temperatures.

In biological membranes, cholesterol generally acts as a modulator of membrane fluidity (Cherry, 1987), and its effect on phospholipid bilayers has been extensively studied by a variety of techniques. Although a comprehensive understanding of the manner in which cholesterol interacts with the bilayer remains to be formulated, many details of these interactions have been made clear in recent years. A number of techniques (laser Raman spectroscopy, FTIR, electron spin resonance, and deuterium NMR) have been used to establish that cholesterol decreases the relative number of gauche conformers when the bilayer is in the liquid-crystalline state and increases the relative number of gauche conformers when the bilayer is in the gel state [cf. Lee and Chapman (1987)]. For example, a study of the effect of cholesterol on 1-palmitoyl-2-oleoylphosphatidylcholine bilayers, using laser Raman spectroscopy, demonstrated that cholesterol caused a decrease in the number of gauche conformers, which resulted in significant ordering of the acyl chains in the liquid-crystalline state (Levin, 1984). Packing of the acyl chains in the bilayer is enhanced as the ratio of gauche to trans conformers is reduced. Cholesterol reduces this ratio and thus augments acyl chain packing, which results in lateral contraction of the bilayer. This "effect" is likely responsible for the observed reduction in bilayer fluidity. More ordered acyl chain packing would also be expected to result in a reduced free volume available for molecular motion in the hydrophobic core of the bilayer.

The effects of cholesterol on lipid bilayer properties were recently studied in this laboratory utilizing the fluorescent membrane probe DPH (Straume & Litman, 1987a,b, 1988). The dynamic fluorescent depolarization of DPH was investigated as a function of mole percent cholesterol and temperature in rhodopsin-containing egg PC vesicles. The results were characterized by a fractional volume parameter, f_V, which represents the volume available to the probe for reorientational motion in the bilayer relative to that available in an unhindered, isotropic environment. This parameter was adopted in order to summarize the relative changes in acyl chain equilibrium order generated by variations in both temperature and bilayer mole percent cholesterol. The value of f_V was found to decrease with increasing cholesterol content and decreasing temperature, suggesting a reduction in free volume available for molecular motion in the hydrophobic region of the bilayer for these conditions. This result is consistent with the increased acyl chain ordering observed in cholesterol-containing bilayers as determined by increased order parameters using other spectroscopic techniques. However, unlike measurements of intramolecular order parameters, the f_V parameter, derived from DPH fluorescence measurements, appears to reflect the consequences of the motional averaging of the ensemble of lipid molecules composing the bilayer on the packing free volume of the hydrocarbon region of the bilayer.

In order to examine the effects of cholesterol and temperature on K_{eq} in terms of differences in the physical state of the lipid bilayer, the present results regarding K_{eq} were compared with the previously obtained f_V data. Over the temperature range 10–37 °C and for bilayer cholesterol levels up to 30 mol %, K_{eq} and f_V have a linear relationship, as shown in Figure 5. It is significant that the relationship between K_{eq} and f_V is maintained regardless of whether the properties of the bilayer are perturbed by changing bilayer composition or temperature. The solid symbols in Figure 5 denote measurements made at 37 °C, and illustrate the isothermal variation in both parameters resulting exclusively from changes in bilayer mole percent cholesterol. Similarly, the variation due to temperature alone for the 0 mol % cholesterol bilayer corresponds to the circles. Within experimental error, these two subsets of the data fall on the best line for all of the data. The correlation between K_{eq} and a parameter which reflects a bulk or global physical property of the lipid bilayer implies that the reduction in K_{eq} with added cholesterol is due to a cholesterol-induced change in the physical state of the lipid bilayer, rather than a specific cholesterol–rhodopsin interaction. The data in Figure 5 demonstrate that whether the composition of the bilayer is isothermally modified or the temperature is varied at a given bilayer composition, the relationship between K_{eq} and bilayer equilibrium order, as quantified by f_V remains unchanged. This observation indicates that f_V should be useful as a normalizing parameter which characterizes bilayer properties with respect to the modulation of integral membrane protein conformational changes and hence protein function. In addition, the observed correlation supports the idea that DPH depolarization reflects a global property of the bilayer rather than a microdomain created by its presence in the bilayer, and indicates that this property is also sensed by rhodopsin as it undergoes a conformational change.

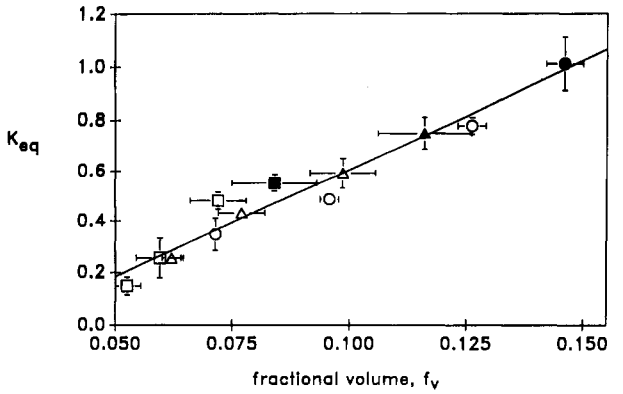

FIGURE 5: K_{eq} versus f_V fractional volume, for 0 (○, ●), 15 (△, ▲), and 30 mol % cholesterol (□, ■) at 10, 20, 30, and 37 °C. Solid symbols denote 37 °C values, and illustrate the variation in both parameters due solely to alteration of bilayer composition. See Discussion for details regarding f_V.

The correlation between K_{eq} and f_V is also consistent with pressure relaxation measurements on bovine ROS disk membranes showing that a positive volume change is involved in the formation of meta II (Lamola et al., 1974; Attwood & Gutfreund, 1980). The reduced packing free volume in the hydrophobic region of the bilayer induced by cholesterol would be expected to reduce the capacity of the bilayer to accommodate an expanded rhodopsin molecular volume. Working between 30 and 150 atm, Attwood and Gutfreund (1980) found that in the meta II state rhodopsin is expanded by 179 Å^3 relative to the meta I state. At 1 atm and a temperature of 1 °C, a pressure of 150 atm was required to reduce K_{eq} by a factor of 2. This is approximately the factor by which 30 mol % cholesterol reduced K_{eq} at all temperatures. Thus, our results demonstrate that isobaric compositional variation of the lipid bilayer can mimic the effects of pressure on meta II production.

The parameter f_V is derived from the behavior of a fluorescent probe which partitions into the hydrophobic core of the bilayer, and thus reflects the packing properties of this portion of the bilayer. The correlation between f_V and K_{eq} gives an indication as to the nature of the protein structural alterations which produce a positive volume change in the meta II state. If this expansion involved only movements normal to the plane of the bilayer and/or rearrangements of the helix-linking regions and carboxyl terminus, it would be relatively unperturbed by alterations in the physical state of the hydrophobic core of the lipid bilayer. However, the results show that the equilibrium concentration of meta II is systematically related to a parameter which characterizes the volume available for molecular motion in the core of the bilayer. This indicates that a significant component of the molecular expansion associated with meta II is radially outward about an axis normal to the membrane, i.e., lateral in nature, and involves motions of the transmembrane α-helices.

FTIR studies demonstrate that meta II is the most structurally altered intermediate in the rhodopsin photobleaching cascade and that significant perturbations in the acyl chain region of unsaturated phospholipids occur on the meta II time scale (DeGrip et al., 1988). FTIR measurements have revealed a number of specific structural alterations characteristic of meta II. These include a change in hydrogen bonding of several carboxyl groups in contact with water (DeGrip et al., 1985) and an increase in β-turn content, presumably in one or more of the cytoplasmic loops (DeGrip et al., 1988). The FTIR results suggest that structural rearrangements in the interior of rhodopsin migrate to the hydrophilic surface of the protein during the meta I-to-meta II transition (DeGrip et al., 1985). This is consistent with the fact that the initial "conformational change" in photolyzed rhodopsin is the 11-cis to all-trans isomerization of the retinal chromophore, which is located approximately in the center of rhodopsin, at the median point of the membrane. The correlation between K_{eq} and f_V indicates that the overall structural changes involved in the formation of meta II are not limited to cytoplasmically exposed domains and involve regions of the protein which interact with the lipid bilayer. This interpretation is supported by the model proposed by DeGrip et al. (1988) which includes changes in the overall shape of rhodopsin due to rearrangements of the α-helices in the meta II intermediate.

The native disk membrane contains a variable amount of cholesterol depending upon its age, with freshly formed disks containing as much as 30 mol % cholesterol (Battaglia & Albert, 1989). However, the complex and multicomponent nature of the native disk lipid system makes it difficult to extrapolate the present results obtained in recombinant bilayers to the native membrane. The differences in K_{eq} with and without cholesterol are small compared with the difference in K_{eq} between the native disk membrane and a recombinant egg PC bilayer. At 37 °C, K_{eq} is about 1 in an egg PC bilayer, and falls to about 0.5 with the addition of 30 mol % cholesterol, but it is over 7 in the disk membrane (Straume et al., 1990). The results of the analysis in terms of ΔH, ΔS, and ΔG_{25} of meta II_{total} relative to meta I provide information as to the thermodynamic basis for these large differences. For meta II_{total} in the native disk membrane, ΔH = 10.6 kcal/mol, ΔS = 37.9 cal/mol·K), and ΔG_{25} = −0.70 (Straume et al., 1990); these values should be compared with those for the reconstituted bilayers in Table IV. The 0 mol % cholesterol bilayer shows that ΔG_{25} goes up by 1.0 kcal/mol, relative to the native disk membrane, due to a reduction in $T\Delta S$ of 3.4 kcal/mol, which offsets a decrease in ΔH of 2.4 kcal/mol. As cholesterol is added to the bilayer, the values of both ΔH and ΔS become more positive. However, since the rise in ΔH is fractionally greater than the growth in ΔS, the result of increasing bilayer mole percent cholesterol is an increase in ΔG_{25}. Thus, it appears that K_{eq} is reduced in these recombinant systems relative to the native disk membrane primarily due to a large decrease in the favorable ΔS for meta II relative to meta I. A number of features of the disk membrane lipid system may be responsible for these differences, notably the asymmetric distribution of lipids between the luminal and cytoplasmic monolayers of the bilayer, the presence of charged headgroups, and the large number of polyunsaturated acyl chains.

In analyzing the kinetic data in terms of the branched meta II model, it was found that cholesterol decreased the equilibrium concentrations of meta II_{fast} and meta II_{slow} in very different ways. Particularly striking are the different effects cholesterol exerted upon ΔH, ΔS, and ΔG_{25} for these two species relative to meta I. The value of ΔH for meta II_{fast} relative to meta I was decreased by a factor of 1.7 by 30 mol % cholesterol, as shown in Table IV. However, ΔG_{25} of meta II_{fast} was increased by 30 mol % cholesterol due to an even larger decrease in ΔS, implying that cholesterol reduced the equilibrium concentration of meta II_{fast} by reducing the gain in conformational degrees of freedom associated with this state relative to meta I. The effect of cholesterol on meta II_{slow} was the reverse of that for meta II_{fast}. The value of ΔH for meta II_{slow} relative to meta I was increased by more than a factor of 4 by 30 mol % cholesterol, while ΔS was increased by a factor of 1.4 (Table IV). This indicates that although cholesterol allowed a higher degree of steric or orientational freedom for meta II_{slow}, relative to the cholesterol-free bilayer, it reduced the equilibrium concentration of this intermediate due to a large increase in relative enthalpy. Cholesterol reduced the equilibrium concentration of both meta II_{fast} and meta II_{slow}, but it accomplished these reductions by increasing the steric or conformational restrictions associated with the former species while decreasing those restrictions associated with the latter species.

A second difference in the effect of cholesterol on meta II_{fast} and meta II_{slow} is shown in Table II. The only process for which $\Delta H^{\ddagger}$ and $\Delta S^{\ddagger}$ are relatively unchanged by addition of cholesterol to the bilayer is that governed by k_1. Inclusion in the bilayer of 30 mol % cholesterol increases the value of $\Delta G^{\ddagger}_{25}$ for this process by less than 0.1 kcal/mol. When compared with the cholesterol-induced changes in $\Delta H^{\ddagger}$ and $\Delta S^{\ddagger}$ for the other dynamic process, this result implies a unique insensitivity to bilayer composition for the formation of the transition state leading from meta I to meta II_{fast}. Although the data do not permit an unambiguous physical explanation of this result, it further defines the diverse effects of cholesterol on meta II_{fast} and meta II_{slow}.

An attractive physical interpretation of the need for two meta II species is that "meta II" represents a single chromophore environment that is linked to a number of energetically distinct protein conformations. In the native ROS disk membrane, the temperature dependence of k_I, k_{II}, k_A, and k_B is consistent with a single pool of meta I decaying through a single activated intermediate into two forms of meta II, while two energetically distinct forms of meta II each pass through a common activated intermediate on the way to meta I (Straume et al., 1990). In these recombinant systems, the specific details which support this interpretation in ROS disk membranes are somewhat altered. The situation in 0 mol % cholesterol is rather similar to that in the disk membrane, as shown in Figure 3A. The nearly superimposable plots of the

two forward rates, k_I and k_A, are consistent with a single pool of meta I decaying via a single transition state to meta II. However, the plots for the reverse rates, k_{II} and k_B are not parallel, which would be consistent with two energetically distinct species decaying via a common activated intermediate. In contrast, in the 30 mol% cholesterol bilayer (Figure 3C), the reverse rates are parallel but vertically displaced, which is consistent with two energetically distinct forms of meta II passing through a common activated intermediate on the way to forming meta I. However, in the 30 mol % bilayer, the two forward rates behave quite differently. The overall similarity in the temperature dependence of the four rate constants in these recombinant bilayers with that found in the native disk membrane indicates that modeling meta II as two states may represent a discrete approximation to a meta II "state" which consists of a distribution of energetically distinct conformational forms (Straume et al., 1990).

Current evidence indicates that meta II is the spectroscopically defined form of rhodopsin which binds and activates G_t, providing the link between photon absorption and the subsequent steps of the visual signal transduction system (Emeis et al., 1982). Therefore, the modulation of meta II formation by varying cholesterol composition represents a significant example of the coupling between membrane protein function and the properties of the lipid bilayer. This finding raises the possibility of biological regulation of membrane protein function via isothermal modification of physical properties of the bilayer through compositional variation. This suggests that altered lipid metabolism could be responsible for some types of visual dysfunction. It has been shown that both the G_t and phosphodiesterase from visually impaired Irish setters function normally (Lolley et al., 1987). The investigators speculated that a rhodopsin abnormality or misorientation of rhodopsin in the bilayer could account for the lack of visual signal transduction. An alternate possibility, suggested by the present work, is that changes in the lipid composition of the ROS disk membrane may have contributed to blocking a membrane-dependent transduction step which occurs before G_t and phosphodiesterase are involved.

Rhodopsin is representative of a class of integral membrane protein receptors which function in signal transduction by activating G-proteins. The modulation of conformational states of rhodopsin by isothermal variation of bilayer composition observed in these studies likely extends to other receptors in this class. In addition, since most activating conformational changes in proteins involve expanded conformations, i.e., opening a cleft to expose a binding site or a channel, these results for rhodopsin should have broad implications for other integral membrane proteins.

Acknowledgments

We thank Dr. Pat Mangan and Deborah Stokes for preparing the recombinant vesicles and performing the associated assays and Dr. M. L. Johnson for the use of his nonlinear least-squares software and much assistance with computer-related aspects of this work.

Registry No. Cholesterol, 57-88-5.

References

Applebury, M. L. (1984) *Vision Res. 24*, 1445–1454.
Applebury, M. L., Zuckerman, D. M., Lamola, A. A., & Jovin, T. M. (1974) *Biochemistry 13*, 3448–3458.
Attwood, P. V. & Gutfreund, H. (1980) *FEBS Lett. 119*, 323–326.
Battaglia, K., & Albert, A. D. (1989) *Biophys. J. 55*, 379a.
Cherry, R. J. (1987) *Biochem. Soc. Trans. 151*, 91–93.
DeGrip, W. J., Gillespie, J., & Rothschild, K. J. (1985) *Biochim. Biophys. Acta 809*, 97–106.
DeGrip, W. J., Gray, D., Gillespie, J., Bovee, P. H. M., Van den Berg, E. M. M., Lugtenberg, J., & Rothschild, K. J. (1988) *Photochem. Photobiol. 48*, 497–504.
Emeis, D., Kuhn, H., Riechert, J., & Hofmann, K. P. (1982) *FEBS Lett. 43*, 29–34.
Jackson, M. L., & Litman, B. J. (1985) *Biochim. Biophys. Acta 812*, 369–376.
Lamola, A. A., Yamane, T., & Zipp, A. (1974) *Biochemistry 13*, 738–745.
Lee, D. C., & Chapman, D. (1987) *Soc. Exp. Biol. 41*, 35–52.
Levin, I. W. (1984) *Adv. Infrared Raman Spectrosc. 11*, 1–48.
Litman, B. J., Kalisky, O., & Ottolenghi, M. (1981) *Biochemistry 20*, 631–634.
Lolley, R. N., Navon, S. E., Fung, B. K. K. & Lee, R. H. (1987) in *Degenerative Retinal Disorders, Clinical and Laboratory Investigation*, pp 269–287, Alan R. Liss. Inc., New York.
Mathews, R. G., Hubbard, P. K., & Wald, G. (1963) *J. Gen. Physiol. 47*, 215–240.
Mitchell, D. C., Straume, M., Miller, J. L., & Litman, B. J. (1989) *Biophys. J. 55*, 380a.
Mitchell, D. C., Kibelbek, J., & Litman, B. J. (1990) *Biophys. J. 57*, 74a.
O'Brien, D. F., Costa, L. F., & Ott, R. A. (1977) *Biochemistry 16*, 1295–1133.
Straume, M., & Litman, B. J. (1987a) *Biochemistry 26*, 5113–5120.
Straume, M., & Litman, B. J. (1987b) *Biochemistry 26*, 5121–5126.
Straume, M., & Litman, B. J. (1988) *Biochemistry 27*, 7723–7733.
Straume, M., Mitchell, D. C., Miller, J. L., & Litman, B. J. (1990) *Biochemistry* (preceding paper in this issue).
Stubbs, G. W., & Litman, B. J. (1978a) *Biochemistry 17*, 215–219.
Stubbs, G. W., & Litman, B. J. (1978b) *Biochemistry 17*, 220–225.